Research on Open-circuit Fault Tolerant Control of Six-phase Permanent Magnet Synchronous Machine Based on Fifth Harmonic Current Injection

Zhifeng Zhang, *Member, IEEE*, Yue Wu, *Student Member, IEEE*, Hequn Su, and Quanzeng Sun

***Abstract*—This paper proposes a novel control approach for fault-tolerant control of dual three-phase permanent magnet synchronous motor (PMSM) under one-phase open-circuit fault. A modified six-phase static coordinate transformation matrix and an extended rotating coordinate transformation matrix are investigated considering the influence of the fifth harmonic space on fault-tolerant control. These mathematical models are further analyzed in the fundamental space and the fifth harmonic space after the fault and to eliminate the coupling between the d-q axis voltage equation in the fundamental wave space and the d-q axis voltage equation in the fifth harmonic space, a secondary rotation coordinate transformation matrix is proposed. To achieve the purpose of reducing torque ripple, the fault-tolerant control method proposed in this paper not only takes the minimum copper loss as the constraint condition, but also injects the fifth harmonic current. The experimental result of current and torque is used to verify the accuracy of fault-tolerant control.**

***Index Terms*—Extended rotating coordinate transformation matrix, Fault-tolerant control, Fifth harmonic current injection, Modified six-phase static coordinate transformation matrix, Dual three-phase permanent magnet synchronous motor, Torque ripple.**

I. INTRODUCTION

IN recent years, with the rapid development of aerospace, ship propulsion, and new energy vehicles, the research on multi-phase permanent magnet synchronous motor (PMSM) has attracted extensive attention [1]-[2]. Compared with three-phase PMSM, multi-phase PMSM has obvious advantages such as low torque ripple, strong fault tolerance, and multiple control resources, which is especially suitable for applications that require high accuracy and strong fault tolerance [3]-[5].

The purpose of fault-tolerant control is that the motor after an open-circuit fault can continue to run and has little change in performance [6]-[12]. Therefore, the optimization and improvement of the fault-tolerant control method is the critical research direction [13].

In [14], a reduced order decoupling matrix is proposed for open-circuit faults of five-phase synchronous motors, but the rotational voltage equation is not symmetric, so this method needs voltage feedforward compensation. In [15], the fault-tolerant operation of asymmetric six-phase induction motor is studied, the correlation between fault current components is analyzed, and the decoupling transformation matrix of fault-tolerant operation is derived. In [16], in order to realize fault-tolerant operation of multiphase motor with open circuit faults, a non-orthogonal reduced order decoupling matrix is proposed. The decoupling matrix deleted the elements related to faults and the amplitude symmetry of the back electromotive force after the fault is realized.

In [17], the one-phase open-circuit fault of the dual three-phase PMSM is analyzed, and the fault-tolerant control is divided into two operation modes, one is loss mode, the other is torque mode. Although this literature achieves the minimum copper loss and the maximum output torque, respectively, it still provides a good help. In [18], not only the five common faults of dual three-phase PMSM are diagnosed, but also a voltage compensation method is used to achieve fault-tolerant control. And the experimental results have proved the effectiveness of the method, but the control method can be improved to reduce copper loss and torque fluctuation. In [19], with the dual d-q axis frame, the open-circuit fault model of dual three-phase PMSM is derived, and fault-tolerant control is achieved by controlling two DC current components. However, this method ignores the influence of harmonic space on fault-tolerant control. In [20], a minimum-copper-loss fault-tolerant control method is proposed for open-circuit fault of dual three-phase PMSM, in which the optimized phase currents are all non-sinusoidal waveforms. However, this method does not optimize the torque ripple.

Manuscript received October 12, 2021; revised January 19, 2022, March 15, 2022, and April 12, 2022; accepted May 23, 2022. date of publication September 25, 2022; date of current version September 18, 2022.

This work was supported by the National Natural Science Foundation of China under Grant 61603263.*(Corresponding author: Yue Wu)*

Zhifeng Zhang is currently an associate professor at School of Electrical Engineering in Shenyang University of Technology. Shenyang 110870, China (e-mail: zzf_sut@126.com).

Yue Wu is currently pursuing the Ph.D. degree in Electrical Engineering from Shenyang University of Technology. Shenyang 110870, China (e-mail: wuyue_95@126.com).

Hequn Su received the M.Sc. degree with the School of Electrical Engineering, Shenyang University of Technology, Shenyang 110870, China (e-mail: 448743982@qq.com).

Quanzeng Sun is currently pursuing the Ph.D. degree in Electrical Engineering from Shenyang University of Technology, Shenyang 110870, China (e-mail: 1074287890@qq.com).

Digital Object Identifier 10.30941/CESTEMS.2022.00041

In [21], the strategy of third harmonic current injection is proposed for the five-phase PMSM with open-circuit fault, which suppresses the second and fourth torque ripple effectively. In [22], the fifth and seventh harmonic currents are injected to improve the torque performance of dual three-phase PMSM. And compared with the traditional third harmonic current injection, this method has the advantages of increasing the output torque of the motor, reducing the torque ripple, and not requiring reconnection of the two isolated neutral points. Therefore, this method provides excellent help for this article.

In the references on the research of one-phase open-circuit fault-tolerant control of multi-phase PMSM, the influence of fundamental wave space and harmonic space on fault-tolerant control is rarely considered at the same time [23-25]. After a one-phase open-circuit fault occurs in dual three-phase PMSM, there is a coupling between the fundamental wave space and the harmonic space. Therefore, on the premise of eliminating the coupling between the fundamental wave space and the harmonic space, it is of great engineering significance to optimize dual three-phase PMSM fault-tolerant control.

The research object of this paper is a dual three-phase PMSM with two sets of windings, which are staggered by 30 electrical degrees in space. There are two main research contents in this paper. Firstly, when a one-phase open-circuit fault occurs in the motor, the mathematical models of the fundamental wave space and the fifth harmonic space are studied on the premise of the influence of the fifth harmonic space on the fault-tolerant control method. Meanwhile, the voltage equations in the fundamental wave space and the harmonic space after decoupling are studied. Secondly, the fault-tolerant control method is optimized to increase the output torque and reduce the torque ripple. The fault-tolerant control method takes the minimum stator copper loss as the constraint condition and injects the fifth harmonic current.

II. Mathematical Model After a One-phase Open-circuit

A. Establish Coordinate Transformation Matrix

The open-circuit fault of the Z-phase winding of the dual three-phase PMSM is taken as the precondition of this paper. The topological structure of the voltage source inverter after fault is shown in Fig. 1. It can be seen from Fig.1 that the neutral point of the inverter is isolated, and the neutral line is not connected to the midpoint of the DC bus voltage.

When the dual three-phase PMSM operates normally to obtain a constant electromagnetic torque, the current in each phase winding is shown in (1), where θ is the rotor position angle, I_m is the current amplitude, i_x is phase currents of the dual three-phase PMSM (x =*A*, *B*, *C*, *X*, *Y*, *Z*).

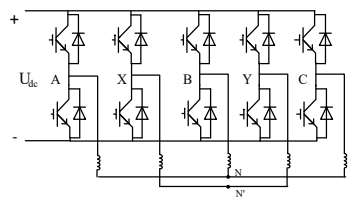

Fig. 1. The topological structure of the voltage source inverter after fault.

$$\begin{aligned} i_A &= I_m\cos(\theta) \\ i_B &= I_m\cos(\theta-2\pi/3) \\ i_C &= I_m\cos(\theta+2\pi/3) \\ i_X &= I_m\cos(\theta-\pi/6) \\ i_Y &= I_m\cos(\theta-5\pi/6) \\ i_Z &= I_m\cos(\theta+\pi/2) \end{aligned} \tag{1}$$

After the Z-phase winding of the motor is open, the relationship between the phase currents is shown in (2). Although the Z-phase winding still has an induced voltage, no current is generated since the Z-phase winding is open. Therefore, the Z-phase winding is no longer involved in the energy conversion of the motor. The motor is in an asymmetrical running state after the fault, so the current needs to be adjusted.

$$i_A+i_B+i_C=0 \qquad i_X+i_Y=0 \tag{2}$$

According to the static coordinate transformation of the dual three-phase PMSM and (2), the zero-sequence component after the fault can be obtained as (3), and the fundamental wave space component can be obtained as shown in (4).

$$z_{01}=\begin{bmatrix}1 & 1 & 1 & 0 & 0\end{bmatrix} \qquad z_{02}=\begin{bmatrix}0 & 0 & 0 & 1 & 1\end{bmatrix} \tag{3}$$

$$\begin{aligned} \alpha_1 &= \begin{bmatrix}1 & -\frac{1}{2} & -\frac{1}{2} & \frac{\sqrt{3}}{2} & -\frac{\sqrt{3}}{2}\end{bmatrix} \\ \beta_1 &= \begin{bmatrix}0 & \frac{\sqrt{3}}{2} & -\frac{\sqrt{3}}{2} & \frac{1}{2} & \frac{1}{2}\end{bmatrix} \\ z_1 &= \begin{bmatrix}1 & -\frac{1}{2} & -\frac{1}{2} & -\frac{\sqrt{3}}{2} & \frac{\sqrt{3}}{2}\end{bmatrix} \end{aligned} \tag{4}$$

In addition, there is a harmonic component z_1, which does not participate in the energy conversion of the motor, but increases the copper loss of the motor. The relationship between α_1, β_1, z_1, z_{01}, z_{02} is shown in (5).

$$\begin{aligned} &\alpha_1^T\beta_1=\alpha_1^T z_1=\alpha_1^T z_{01}=\alpha_1^T z_{02}=0 \\ &\beta_1^T z_1=\beta_1^T z_{01}=\beta_1^T z_{02}=0 \\ &z_1^T z_{01}=z_1^T z_{02}=z_{01}^T z_{02}=0 \end{aligned} \tag{5}$$

Since the motor has an open-circuit fault, the relationship between β_1 and z_{02} is no longer orthogonal to obtain a vector transformation matrix suitable for a one-phase open-circuit [14], [16], [22]. To satisfy (5), β_1 changes to β' and the static coordinate transformation matrix in the fundamental wave space is modified to obtain the following matrix:

$$T_{1s}=\frac{1}{3}\begin{bmatrix}\alpha_1\\ \beta'\\ z_1\\ z_{01}\\ z_{02}\end{bmatrix}=\frac{1}{3}\begin{bmatrix}1 & -\frac{1}{2} & -\frac{1}{2} & \frac{\sqrt{3}}{2} & -\frac{\sqrt{3}}{2}\\ 0 & \frac{\sqrt{3}}{2} & -\frac{\sqrt{3}}{2} & 0 & 0\\ 1 & -\frac{1}{2} & -\frac{1}{2} & -\frac{\sqrt{3}}{2} & \frac{\sqrt{3}}{2}\\ 1 & 1 & 1 & 0 & 0\\ 0 & 0 & 0 & 1 & 1\end{bmatrix} \tag{6}$$

The rotating coordinate matrix of the fundamental wave

space can be expressed as (7).

$$C_{1r}(\theta)=\begin{bmatrix}\cos(\theta) & \sin(\theta) & 0 & 0 & 0\\ -\sin(\theta) & \cos(\theta) & 0 & 0 & 0\\ 0 & 0 & 1 & 0 & 0\\ 0 & 0 & 0 & 1 & 0\\ 0 & 0 & 0 & 0 & 1\end{bmatrix} \tag{7}$$

Similarly, the static coordinate transformation matrix and the rotating coordinate transformation matrix of the fifth harmonic space can be obtained as (8) and (9).

$$T_{5s}=\frac{1}{3}\begin{bmatrix}\alpha_5\\ \beta_5\\ z_5\\ z_{03}\\ z_{04}\end{bmatrix}=\frac{1}{3}\begin{bmatrix}1 & -\frac{1}{2} & -\frac{1}{2} & -\frac{\sqrt{3}}{2} & \frac{\sqrt{3}}{2}\\ 0 & -\frac{\sqrt{3}}{2} & \frac{\sqrt{3}}{2} & 0 & 0\\ 1 & -\frac{1}{2} & -\frac{1}{2} & \frac{\sqrt{3}}{2} & -\frac{\sqrt{3}}{2}\\ 1 & 1 & 1 & 0 & 0\\ 0 & 0 & 0 & 1 & 1\end{bmatrix} \tag{8}$$

$$C_{5r}(\theta)=\begin{bmatrix}\cos(5\theta) & \sin(5\theta) & 0 & 0 & 0\\ -\sin(5\theta) & \cos(5\theta) & 0 & 0 & 0\\ 0 & 0 & 1 & 0 & 0\\ 0 & 0 & 0 & 1 & 0\\ 0 & 0 & 0 & 0 & 1\end{bmatrix} \tag{9}$$

B. Establish Mathematical Model After Fault

When the Z-phase winding of dual three-phase PMSM is open-circuit, the stator voltage equation of the remaining five phases in the static coordinate system can be expressed as follows:

$$U_{5s}=R_{5s}I_{5s}+d\psi_{5s}/dt \tag{10}$$

Where U_{5s} is the stator voltage matrix, R_{5s} is the resistance, I_{5s} is the stator current matrix, ψ_{5s} which is the stator flux linkage matrix, where $R_{5s}=R_s\times E_{5\times5}$, $E_{5\times5}$ is the unit matrix.

The stator flux linkage equation can be expressed as:

$$\psi_{5s}=L_{5s}I_{5s}+\psi_{5m} \tag{11}$$

Where L_{5s} is the stator inductance matrix and ψ_{5m} is the permanent magnet flux linkage of the remaining five phases.

Through the modified coordinate transformation matrix (6) and (7), the voltage equation and the flux linkage equation of the fundamental wave space in the rotating coordinate system can be obtained. The direction of Z-phase winding is selected in the direct axis direction, and the fundamental wave voltage equation after transformation can be expressed as (12). The transformed fundamental wave flux linkage matrix can be expressed as (13). Similarly, through (8), (9), and (14), the voltage equation and flux linkage equation in the fifth harmonic space can be obtained (only the subscript is different, so it is not listed repeatedly).

$$U_{(dqz)1}=T_1(\theta)\cdot U_{5s}=R_{5s}I_{(dqz)1}+\frac{d\psi_{(dqz)1}}{dt}-\omega\psi_{(dqz)1} \tag{12}$$

$$\psi_{(dqz)1}=T_1(\theta)\cdot(L_{5s}I_{5s}+\psi_{5m})=L_{(dqz)1}I_{(dqz)1}+\psi_{(dqm)1} \tag{13}$$

$$\begin{aligned}T_1(\theta)&=C_{1r}(\theta)\cdot T_{1s}\\ T_5(\theta)&=C_{5r}(\theta)\cdot T_{5s}\end{aligned} \tag{14}$$

The inductance matrix in the rotating coordinate system of the fundamental wave space and the fifth harmonic space can be expressed as (15) and (16). The permanent magnet flux linkage matrix of the fundamental wave space and the fifth harmonic space can be expressed as (17) and (18). When substituting (15)-(18) into (12) and (13), the stator voltage matrix in the rotating coordinate system of the fundamental wave space and the fifth harmonic space can be obtained as (19), (20).

$$L_{(dqz)1}=L_{m1}\begin{bmatrix}\frac{9+3\cos(2\theta)}{4} & \frac{-3\sin(2\theta)}{4} & 0 & 0 & \frac{3\sin(\theta)}{4}\\ \frac{-3\sin(2\theta)}{4} & \frac{9-3\cos(2\theta)}{4} & 0 & 0 & \frac{3\cos(\theta)}{4}\\ 0 & 0 & 0 & 0 & 0\\ 0 & 0 & 0 & 0 & 0\\ \sin(\theta) & \cos(\theta) & 0 & 0 & \frac{1}{2}\end{bmatrix}+L_{m5}\begin{bmatrix}\frac{3-3\cos(2\theta)}{4} & \frac{3\sin(2\theta)}{4} & 0 & 0 & \frac{-3\sin(\theta)}{4}\\ \frac{3\sin(2\theta)}{4} & \frac{3+\cos(2\theta)}{4} & 0 & 0 & \frac{-3\cos(\theta)}{4}\\ 0 & 0 & 3 & 0 & 0\\ 0 & 0 & 0 & 0 & 0\\ -\sin(\theta) & -\cos(\theta) & 0 & 0 & \frac{1}{2}\end{bmatrix} \tag{15}$$

$$L_{(dqz)5}=L_{m1}\begin{bmatrix}\frac{3/4-3\cos(10\theta)}{4} & \frac{3\sin(10\theta)}{4} & 0 & 0 & \frac{-3\sin(5\theta)}{4}\\ \frac{3\sin(10\theta)}{4} & \frac{3+\cos(10\theta)}{4} & 0 & 0 & \frac{-3\cos(5\theta)}{4}\\ 0 & 0 & 3 & 0 & 0\\ 0 & 0 & 0 & 0 & 0\\ -\sin(5\theta) & -\cos(5\theta) & 0 & 0 & \frac{1}{2}\end{bmatrix}+L_{m5}\begin{bmatrix}\frac{9+3\cos(10\theta)}{4} & \frac{-3\sin(10\theta)}{4} & 0 & 0 & \frac{3\sin(5\theta)}{4}\\ \frac{-3\sin(10\theta)}{4} & \frac{9-3\cos(10\theta)}{4} & 0 & 0 & \frac{3\cos(5\theta)}{4}\\ 0 & 0 & 0 & 0 & 0\\ 0 & 0 & 0 & 0 & 0\\ \sin(5\theta) & \cos(5\theta) & 0 & 0 & \frac{1}{2}\end{bmatrix} \tag{16}$$

$$\psi_{5m1}=\psi_{m1}\begin{bmatrix}\frac{-(\sin 2\theta)}{4}\\ \frac{3-(\cos 2\theta)}{4}\\ 0\\ 0\\ 0\end{bmatrix}+\psi_{m5}\begin{bmatrix}\frac{-(\sin 5\theta\cdot\cos\theta)}{2}\\ \frac{(\sin 5\theta\cdot\sin\theta)}{2}\\ 0\\ 0\\ 0\end{bmatrix} \tag{17}$$

$$\psi_{5m5}=\psi_{m1}\begin{bmatrix}\frac{-5(\cos 5\theta\cdot\sin\theta)}{2}\\ \frac{5(\sin 5\theta\cdot\sin\theta)}{2}\\ 0\\ 0\\ 0\end{bmatrix}+\psi_{m5}\begin{bmatrix}\frac{-5(\sin 10\theta)}{4}\\ \frac{15/-5(\cos 10\theta)}{4}\\ 0\\ 0\\ 0\end{bmatrix} \tag{18}$$

$$\begin{bmatrix}u_{d1}\\ u_{q1}\end{bmatrix}=R_s\begin{bmatrix}i_{d1}\\ i_{q1}\end{bmatrix}+\begin{bmatrix}L_{d1}\\ L_{q1}\end{bmatrix}M_1(\theta)\frac{d}{dt}\begin{bmatrix}i_{d1}\\ i_{q1}\end{bmatrix}-\begin{bmatrix}L_{q1}\\ -L_{d1}\end{bmatrix}M_1(\theta)\omega\begin{bmatrix}i_{q1}\\ -i_{d1}\end{bmatrix}+\omega\psi_{m1}N_1(\theta)+\begin{bmatrix}\Delta u_{d1}\\ \Delta u_{q1}\end{bmatrix} \tag{19}$$

$$\begin{bmatrix}u_{d5}\\ u_{q5}\end{bmatrix}=R_s\begin{bmatrix}i_{d5}\\ i_{q5}\end{bmatrix}+\begin{bmatrix}L_{d1}\\ L_{q1}\end{bmatrix}M_5(\theta)\frac{d}{dt}\begin{bmatrix}i_{d5}\\ i_{q5}\end{bmatrix}-5\begin{bmatrix}L_{q5}\\ -L_{d5}\end{bmatrix}M_5(\theta)\omega\begin{bmatrix}i_{q5}\\ -i_{d5}\end{bmatrix}+5\omega\psi_{m1}N_5(\theta)+\begin{bmatrix}\Delta u_{d5}\\ \Delta u_{q5}\end{bmatrix} \tag{20}$$

$$M_1(\theta)=\begin{bmatrix}3/4+\cos(2\theta)/4 & -\sin(2\theta)/4\\ -\sin(2\theta)/4 & 3/4-\cos(2\theta)/4\end{bmatrix} \tag{21}$$

$$N_1(\theta)=\begin{bmatrix}-\sin(2\theta)/4\\ 3/4-\cos(2\theta)/4\end{bmatrix} \tag{22}$$

$$M_5(\theta)=\begin{bmatrix}3/4+\cos(10\theta)/4 & -\sin(10\theta)/4\\ -\sin(10\theta)/4 & 3/4-\cos(10\theta)/4\end{bmatrix} \tag{23}$$

$$N_5(\theta)=\begin{bmatrix}-\sin(10\theta)/4\\ 3/4-\cos(10\theta)/4\end{bmatrix} \tag{24}$$

Where L_{m1} is the stator inductance at the fundamental wave and L_{m5} is the stator inductance at the fifth harmonic. ψ_{5m1} is the permanent magnet flux linkage of the remaining five phases at the fundamental wave. ψ_{5m5} is the permanent magnet flux linkage of the remaining five phases at the fifth harmonic. ω is dual three-phase PMSM electrical angular speed. u_{d1} and u_{q1} are d-q axis voltages at the fundamental wave. i_{d1} and i_{q1} are d-q axis currents at the fundamental wave. L_{d1} and L_{q1} are d-q axis currents at the fundamental wave. L_{d1} and L_{q1} are d-q axis inductances at the fundamental wave.

When the dual three-phase PMSM has a one-phase open-circuit fault, the winding structure is no longer symmetrical. According to (19) and (20), it can be found that there is still a coupling relationship between the voltage equations in the rotating coordinate system, which is related to the rotor position angle. It is necessary to multiply the inverse matrix of $M_1(\theta)$ and $M_5(\theta)$ on both sides of (19) and (20), respectively, to eliminate the influence of nonlinear factors caused by rotor position angle and realize the decoupling control of dual three-phase PMSM under fault condition, which can be obtained as (25) and (26). The voltage increment in (19) and (20) can be regarded as an interference term whose magnitude varies periodically with the position of the rotor. After calculating by (27) and (28), the feed-forward method is used to compensate, which can make the mathematical model more accurate. If the voltage increment is ignored, (19) and (20) are the voltage equations of a dual three-phase PMSM in normal operation.

$$\begin{bmatrix}u_{m1}\\ u_{n1}\end{bmatrix}=M_1(\theta)^{-1}\cdot\begin{bmatrix}u_{d1}\\ u_{q1}\end{bmatrix} \tag{25}$$

$$\begin{bmatrix}u_{m5}\\ u_{n5}\end{bmatrix}=M_5(\theta)^{-1}\cdot\begin{bmatrix}u_{d5}\\ u_{q5}\end{bmatrix} \tag{26}$$

$$\begin{bmatrix}\Delta u_{d1}\\ \Delta u_{q1}\end{bmatrix}=\omega L_{m5}\begin{bmatrix}3/4-3\cos(2\theta)/4 & 3\sin(2\theta)/4\\ 3\sin(2\theta)/4 & 3/4+\cos(2\theta)/4\end{bmatrix}\cdot\begin{bmatrix}i_{d1}\\ i_{q1}\end{bmatrix}+\omega\psi_{m5}\begin{bmatrix}-(\sin 5\theta\cdot\cos\theta)/2\\ (\sin 5\theta\cdot\sin\theta)/2\end{bmatrix} \tag{27}$$

$$\begin{bmatrix}\Delta u_{d5}\\ \Delta u_{q5}\end{bmatrix}=\omega L_{m1}\begin{bmatrix}3/4-3\cos(10\theta)/4 & 3\sin(10\theta)/4\\ 3\sin(10\theta)/4 & 3/4+\cos(10\theta)/4\end{bmatrix}\cdot\begin{bmatrix}i_{d5}\\ i_{q5}\end{bmatrix}+\omega\psi_{m1}\begin{bmatrix}-5(\cos 5\theta\cdot\sin\theta)/2\\ 5(\sin 5\theta\cdot\sin\theta)/2\end{bmatrix} \tag{28}$$

C. Calculate electromagnetic torque and harmonic injection ratio

When the current constraint is constant, the electromagnetic torque is equal to the partial derivative of the magnetic common energy with respect to the mechanical angle of the rotor. The electromagnetic torque can be calculated from (29).

$$T_e=p(\frac{1}{2}I_{5s}^T\frac{\partial L_{5s}}{\partial\theta}I_{5s}+I_s^T\frac{\partial\psi_{5m}}{\partial\theta})=pI_s^T\frac{\partial\psi_{5m}}{\partial\theta} \tag{29}$$

The electromagnetic torque generated by the fundamental wave current is:

$$T_{e1}=p\psi_{m1}(3I_{q1}+\frac{3}{2}I_{o2}\cos\theta)+p\psi_{m5}[\frac{15}{2}(\sin 4\theta-\sin 6\theta)I_{d1}-\frac{15}{2}(\cos 4\theta+\cos 6\theta)I_{q1}-15\sin 5\theta\cdot I_{z1}+\frac{15}{2}\cos\theta\cdot I_{o2}] \tag{30}$$

The electromagnetic torque generated by the fifth harmonic current is:

$$T_{e5}=p\psi_{m1}[-\frac{3}{2}(\sin 4\theta+\sin 6\theta)I_{d5}-\frac{3}{2}(\cos 4\theta+\cos 6\theta)I_{q5}-3\sin\theta\cdot I_{z5}+\frac{3}{2}\cos\theta\cdot I_{o4})]+p\psi_{m5}(15I_{q5}+\frac{15}{2}\cos 5\theta) \tag{31}$$

According to the superposition principle, the total electromagnetic torque is (32).

$$T_e=T_{e1}+T_{e5} \tag{32}$$

According to (30), (31), and (32), the expressions of the average torque and each torque ripple can be obtained as shown in (33).

In the control process, the space vector control strategy with I_{d1}=I_{d5}=0 is used, and there are six control components remaining: I_{q1}, I_{q5}, I_{z1}, I_{z5}, I_{o2}, I_{o4}. I_{q1} and I_{q5} are the current components in the rotating coordinate system. The two zero-sequence components I_{o2} and I_{o4} are always controlled to zero. When only fundamental wave space is considered, the other two generalized zero-sequence components I_{z1} and I_{z5} are not involved in electromechanical energy conversion [26]. However, when the fifth harmonic is considered, I_{z1} and I_{z5} can be optimized to achieve the minimum copper loss. The average torque and torque ripple can be controlled by adjusting I_{q1} and I_{q5}. Through the expressions of the fourth and sixth torque ripple in (33), it can be seen that when the injected fifth harmonic current and the fundamental wave current satisfy the harmonic injection ratio calculated by (34), the sum of the fourth and sixth torque ripple is zero.

$$\begin{aligned}
t_0 &= 3p(\psi_{m1}\cdot I_{q1}+5\cdot\psi_{m5}\cdot I_{q5})\\
t_1 &= \frac{3}{2}p\psi_{m1}[(I_{o2}+I_{o4})\cos\theta-2I_{z5}\sin\theta]\\
t_4 &= -\frac{3}{2}p\psi_{m1}(I_{d5}\sin 4\theta+I_{q5}\cos 4\theta)\\
&\quad+\frac{15}{2}p\psi_{m5}(I_{d1}\sin 4\theta-I_{q1}\cos 4\theta)\\
t_5 &= \frac{15}{2}p\psi_{m5}[(I_{o2}+I_{o4})\cos 5\theta-2I_{z1}\sin 5\theta]\\
t_6 &= -\frac{3}{2}p\psi_{m1}(I_{d5}\sin 6\theta+I_{q5}\cos 6\theta)\\
&\quad-\frac{15}{2}p\psi_{m5}(I_{d1}\sin 6\theta+I_{q1}\cos 6\theta)
\end{aligned} \tag{33}$$

$$k=5\frac{\psi_{m5}}{\psi_{m1}}=\frac{E_5}{E_1} \tag{34}$$

III. The Principle Of Minimum Copper Loss Under The Fifth Harmonic Current Injection

In the control process, the vector control strategy with I_{d1}=I_{d5}=0 is used. According to the superposition principle, the copper loss is generated by the fundamental wave current and the fifth harmonic current [26]. The copper loss under fundamental wave current is (35). Similarly, the copper loss under the fifth harmonic current is (36). The total copper loss of the motor is (37).

$$P_{cu1}=I_{5s}^{T}I_{5s}R_s=R_s\{I_{q1}^2[\frac{9}{2}+\frac{3}{2}\cos(2\theta)]+3I_{z1}^2+3I_{o1}^2+\frac{9}{2}I_{o2}^2\} \tag{35}$$

$$P_{cu5}=R_s\{I_{q5}^2[\frac{9}{2}+\frac{3}{2}\cos(10\theta)]+3I_{z5}^2+3I_{o3}^2+\frac{9}{2}I_{o4}^2\} \tag{36}$$

$$P_{cu}=P_{cu1}+P_{cu5} \tag{37}$$

The zero-sequence current components are always controlled to zero in the control process, and the generalized zero-sequence components I_{z1} and I_{z5} are also controlled to zero by the PI controller. Therefore, the minimum copper loss can be obtained, and it can be ensured that the first and fifth torque ripples are also zero. The new fundamental wave fault-tolerant current is (38). The new fifth harmonic fault-tolerant current is (39). The new fault- tolerant current is obtained by superposition of the fundamental wave current and the injected fifth harmonic current, as shown in (40).

$$\begin{aligned}
i_{A1} &= I_{m1}\cos\theta\\
i_{B1} &= 1.803\,\mathrm{I}_{m1}\cos(\theta-106.1°)\\
i_{C1} &= 1.803\,\mathrm{I}_{m1}\cos(\theta+106.1°)\\
i_{X1} &= 0.886I_{m1}\cos\theta\\
i_{Y1} &= -0.886I_{m1}\cos\theta
\end{aligned} \tag{38}$$

$$\begin{aligned}
i_{A5} &= I_{m5}\cos 5\theta\\
i_{B5} &= -0.886I_{m5}\cos 5\theta\\
i_{C5} &= 0.886I_{m5}\cos 5\theta\\
i_{X5} &= -1.803\,\mathrm{I}_{m5}\cos(5\theta+106.1°)\\
i_{Y5} &= -1.803\,\mathrm{I}_{m5}\cos(5\theta-106.1°)
\end{aligned} \tag{39}$$

$$\begin{aligned}
i_A &= I_{m1}\cos\theta-I_{m5}\cos 5\theta\\
i_B &= 1.803\,\mathrm{I}_{m1}\cos(\theta-106.1°)-0.886I_{m5}\cos 5\theta\\
i_C &= 1.803\,\mathrm{I}_{m1}\cos(\theta+106.1°)+0.886I_{m5}\cos 5\theta\\
i_X &= 0.886I_{m1}\cos\theta-1.803\,\mathrm{I}_{m5}\cos(5\theta+106.1°)\\
i_Y &= -0.886I_{m1}\cos\theta-1.803\,\mathrm{I}_{m5}\cos(5\theta-106.1°)
\end{aligned} \tag{40}$$

IV. Simulation Analysis

Based on the analysis of the previous three parts, the fault tolerant control algorithm of a six-phase PMSM after a one phase open circuit fault is simulated and analyzed. The control block diagram of the fault tolerant control system is shown in Fig. 2. The simulated dual three-phase PMSM parameters are shown in TABLE I. The precondition of the simulation is the speed command of 1000 r/min with 40 Nm load.

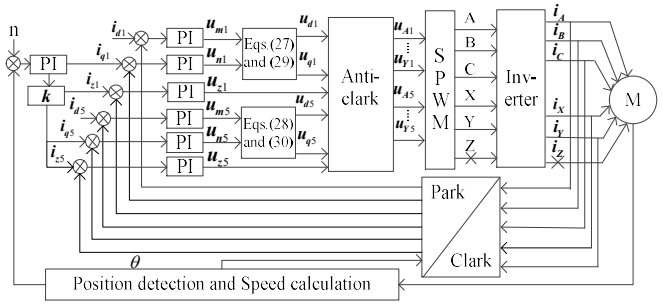

Fig. 2. Fault tolerant control of the dual three-phase PMSM

TABLE I
PARAMETERS OF DUAL THREE-PHASE PMSM

Parameters	Value
R	0.002Ω
L_{m1}	360μH
L_{m5}	90μH
Ψ_{m1}	0.092Wb
Ψ_{m5}	0.0023Wb
Pole pairs	4
Moment of inertia	0.02kg·m^2
Rated speed	3000r/min
Rated torque	98Nm

The dual three-phase PMSM runs under normal operating

state during 0.1-0.2s, and runs under fault operating state during 0.2-0.3s. During 0.4-0.5s, the fault-tolerant control method without the fifth harmonic injection and with fifth harmonic injection are introduced. Fig. 3 and Fig. 4 respectively show the current waveform and torque waveform under four operating states.

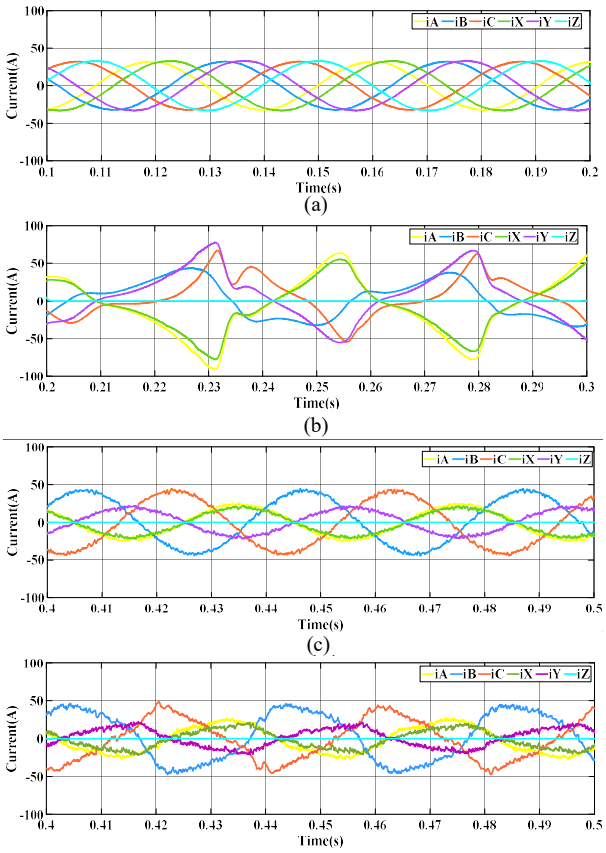

Fig. 3. Current waveform of the dual three-phase PMSM under (a) normal operating state (b) the open-circuit fault of Z-phase (c) fault-tolerant control method without fifth harmonic current injection (d) fault-tolerant control method with fifth harmonic current injection.

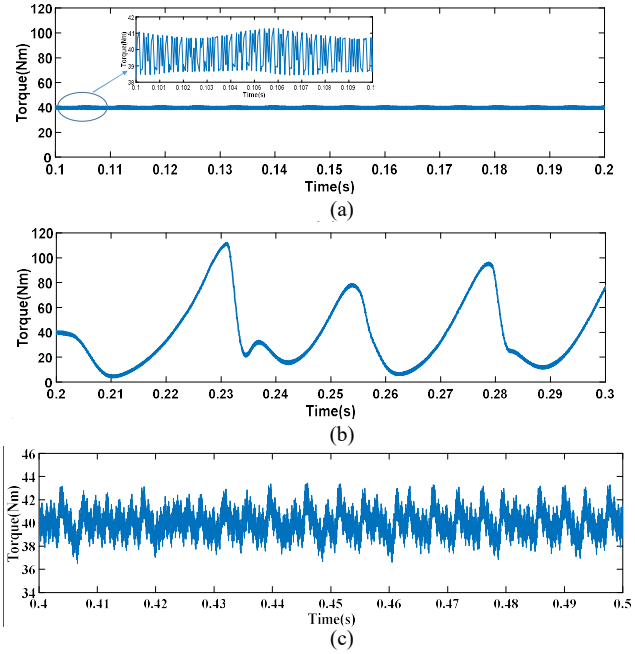

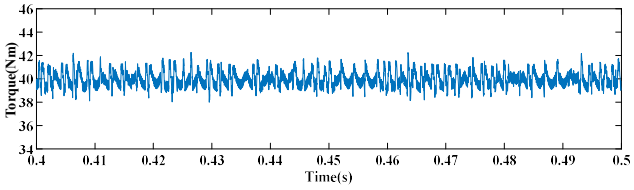

Fig. 4. Torque waveform of the dual three-phase PMSM under (a) normal operating state (b) the open-circuit fault of Z-phase (c) fault-tolerant control method without fifth harmonic current injection (d) fault-tolerant control method with fifth harmonic current injection

To evaluate the performance of the two fault-tolerant methods, the following indexes are defined:

1) Torque ripple: comparison of instantaneous value and average value.

$$T_{e\_ripple}=\sqrt{\frac{1}{n}\sum_{i=1}^{n}(T_{e\_i}-T_{e\_av})^2} \tag{41}$$

2) Torque ripple change rate: ratio of torque ripple to normal torque

$$\Delta T_e=\frac{T_{e\_ripple}}{T_{e\_normal}}\times 100\% \tag{42}$$

As shown in Fig. 3(a), the amplitude of the six-phase current is the same and current waveforms present sinusoidal. From the partial enlarged view of Fig. 4(a), the electromagnetic torque changes smoothly, and the torque ripple calculated is 0.94 Nm by (41). When the Z-phase occurs open-circuit fault at 0.2s, it can be seen from Fig. 3(b) that the Z-phase current has a sudden change to zero, and the other phase current waveforms are distorted. Since no fault-tolerant control method is introduced, it can be seen from Fig. 4(b) that the electromagnetic torque changes greatly, and the torque ripple is 26.78Nm, which will seriously affect the performance of the dual three-phase PMSM. Since the dual three-phase motor control system introduces fault-tolerant control method, the amplitudes of each phase current shown in Fig. 3(c) and Fig. 3(d) are basically the same except for the Z-phase. Compared with Fig. 3(c), the phase current waveform of Fig. 3(d) has a certain degree of distortion, which is the reason for the injection of the fifth current harmonics. Although the performance of the phase current deteriorates, it can be obtained that the change of electromagnetic torque is significantly reduced through Fig. 4(c) and Fig. 4(d). The torque ripple is reduced from 3.86 Nm to 1.88 Nm.

The two performance indexes of the dual three-phase PMSM under four operating states are shown in TABLE II. It can be seen from the TABLE II that the torque change rate of the fault-tolerant control method with the fifth harmonic injection is 4.7%. The torque change rate of the fifth harmonic injection method is 62.25% and 5% lower than the torque change rate of the fault operating state and without the fifth harmonic injection method, respectively. Therefore, the two performance indexes of fault-tolerant control method with harmonic injection are better than those of fault-tolerant control method without harmonic injection.

The comparative analysis of the two methods is based on the principle of minimum copper consumption control strategy, that is, the control strategy that maintains $I_{d1}=I_{d5}=I_{z1}=I_{z5}=0$.

The motor can run smoothly after the fault-tolerant operation, which verifies the correctness of the method.

TABLE II
PERFORMANCE INDEX

Performance	Normal	Fault	Without current injection	With current injection
$T_{e\text{-}ripple}$	0.94	26.78	3.86	1.88
ΔT_e	2.3%	66.95%	9.7%	4.7%

V. Experimental Analysis

The experiment of the dual three-phase PMSM is carried out to verify the correctness of the mathematical model and the fault-tolerant control method of the theoretical and simulation analysis. The experimental motor parameters are the same as the simulated motor parameters, and the experimental platform is shown in Fig. 5. The hardware platform is constructed based on (DSP) TMS320F28335, and the sampling frequency is 10 kHz.

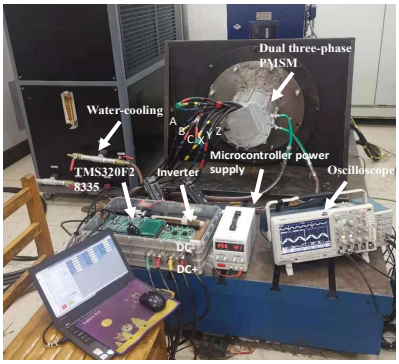

Fig. 5. Experimental platform.

Test 1: Compare the current changes of two fault-tolerant control methods under the speed command of 1500 rpm with 30 Nm load.

When the Z-phase of the motor has an open-circuit fault, the fault current is shown in Fig. 6.

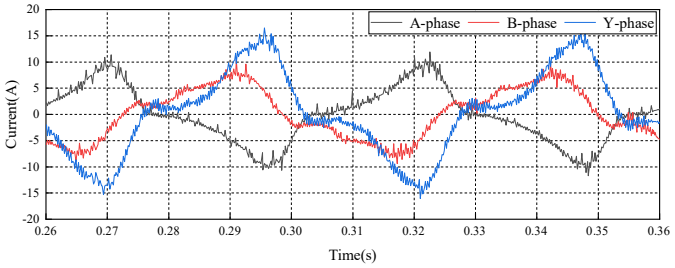

Fig. 6. Open-circuit fault current waveform.

The current waveform and the phase current total harmonic distortion (THD) under the two fault-tolerant control methods are shown in Fig. 7 and Fig. 8. It can be seen from the Fig. 7(a) and Fig. 8(a) that the fault-tolerant current has some distortion with the fifth harmonic current injection.

One of the phases current is selected to calculate THD. Fig. 7(b) and Fig. 8(b) are FFT (Fast Fourier Transformation) analyses of B-phase current under without fifth harmonic injection and with fifth harmonic injection, THD are 8.36% and 17.68%, respectively. The degree of distortion of B-phase current with the fifth harmonic injection is acceptable. Fig. 9(a) is the back-electromotive force(back-EMF) waveform with fifth harmonic current injection, and Fig. 9(b) is the spectrum of back-EMF. It can be seen from Fig. 8(b) and Fig. 9(b) that the fifth harmonic content increases significantly.

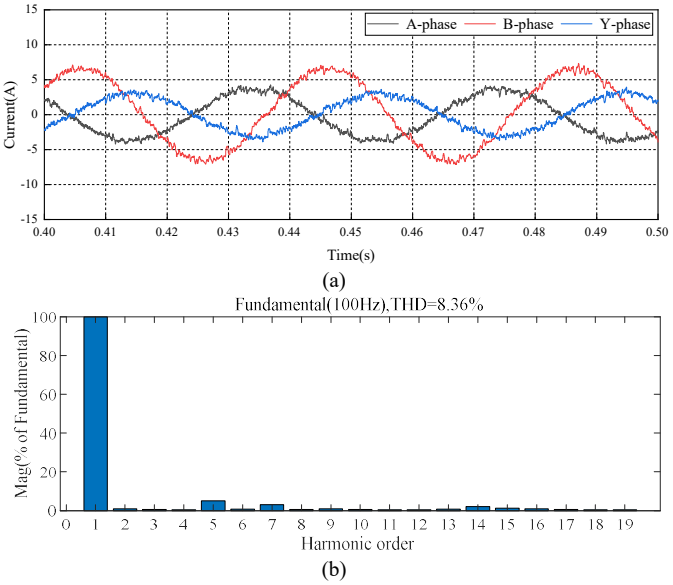

Fig. 7. (a) Fault-tolerant control current waveform without fifth harmonic current injection and (b) THD of B-phase current.

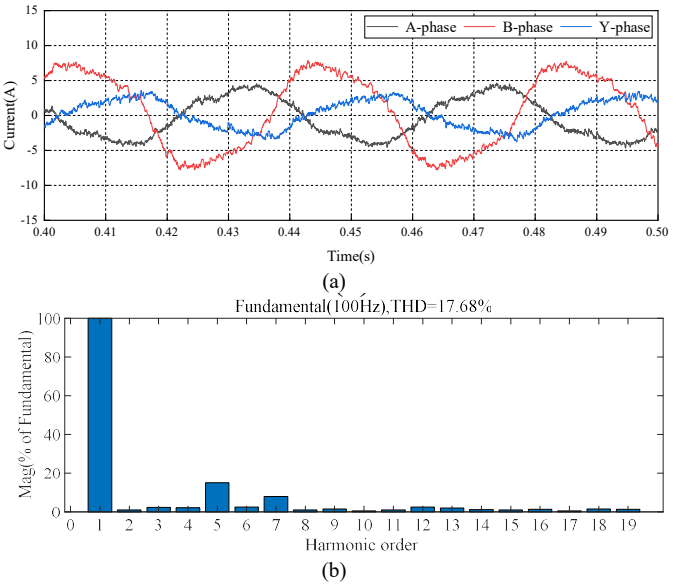

Fig. 8. (a) Fault-tolerant control current waveform with fifth harmonic current injection and (b) THD of B-phase current.

Test 2: Compare the torque waveform of two fault-tolerant control method under the speed command of 1000 rpm with 30 Nm load.

Fig. 10(a) shows the torque waveform under the fault-tolerant control without fifth harmonic current injection. It can be seen from the Fig. 10(a) that torque ripple is about 4.5 Nm. Fig. 10(b) shows the torque waveform under the fault-tolerant control with fifth harmonic current injection. It can be seen from the Fig. 10(b) that the dual three-phase PMSM runs smoothly, and the torque ripple is about 2.5 Nm.

The torque ripple under different speeds (from 0.1 to 1.0 p.u. of the rated speed) with 98Nm load. It can be seen from the Fig. 11 that torque ripple with fifth harmonic current injection is

much lower than that without fifth harmonic current injection in the whole speed range. The torque ripple of the two fault-tolerant control methods hardly fluctuates with the change of speed, and the average torque ripples of the two methods are 4.4 Nm and 2.2 Nm, respectively, which proves the effectiveness of the proposed method.

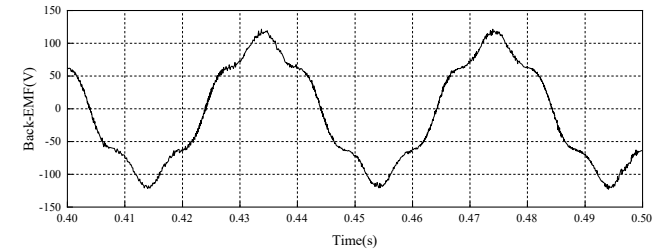

(a)

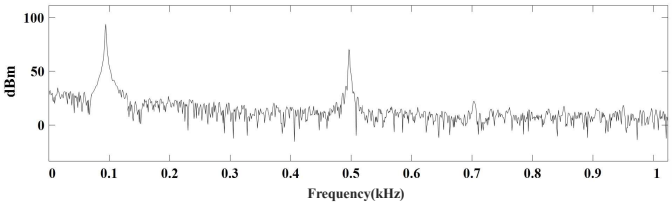

(b)

Fig. 9. (a) Fault-tolerant control back-EMF waveform with fifth harmonic current injection and (b) Spectrum of back-EMF.

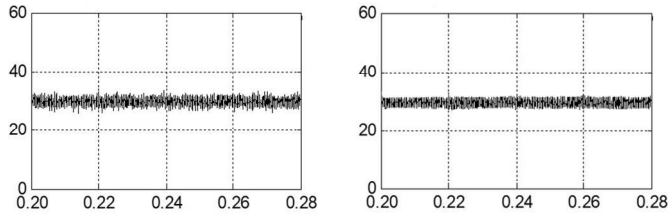

(a) (b)

Fig. 10. (a) Fault-tolerant control torque waveform without fifth harmonic current injection and (b) with fifth harmonic current injection.

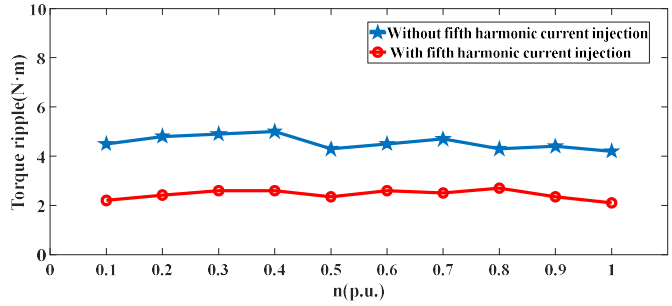

Fig. 11. Torque ripple at 98 Nm load under different speed commands.

VI. Conclusions

In this paper, the fault-tolerant control of dual three-phase PMSM is analyzed and studied in depth. Simulations and experiments prove that the fault-tolerant control method with harmonic current injection is better than the fault-tolerant control method without harmonic current injection. The innovations of the novel fault-tolerant control method include:

1) The modified static coordinate transformation matrix and rotating coordinate transformation matrix are derived;

2) Through these two new coordinate transformation matrices, the voltage equations, flux linkage equation and torque equation in the fundamental wave space and the fifth harmonic space after the fault are derived;

3) The coupling between the d-q axis voltage equation of the fundamental wave and the d-q axis voltage equation of the fifth harmonic after the fault is eliminated;

4) The fault-tolerant control method injects the fifth harmonic current on the basis of the minimum stator copper loss as the constraint condition. Simulation results and experimental results prove that torque ripple can be effectively reduced.

In the future, there are still several aspects that need to be researched. Firstly, the fault diagnosis method combined with fault-tolerant control needs to be studied; secondly, the fault-tolerant control method when a two-phase open-circuit occurs in a dual three-phase PMSM needs to be studied; finally, the fault-tolerant control method of the dual three-phase PMSM with non-isolated neutral point needs to be studied.

VII. Appendix

The original inductance matrix can be expressed as follows:

$$L_{5s}=L_{m1}\begin{bmatrix} 1 & -\frac{1}{2} & -\frac{1}{2} & \frac{\sqrt{3}}{2} & -\frac{\sqrt{3}}{2} \\ -\frac{1}{2} & 1 & -\frac{1}{2} & 0 & \frac{\sqrt{3}}{2} \\ -\frac{1}{2} & -\frac{1}{2} & 1 & -\frac{\sqrt{3}}{2} & 0 \\ \frac{\sqrt{3}}{2} & 0 & -\frac{\sqrt{3}}{2} & 1 & -\frac{1}{2} \\ -\frac{\sqrt{3}}{2} & \frac{\sqrt{3}}{2} & 0 & -\frac{1}{2} & 1 \end{bmatrix}+ L_{m5}\begin{bmatrix} 1 & -\frac{1}{2} & -\frac{1}{2} & -\frac{\sqrt{3}}{2} & \frac{\sqrt{3}}{2} \\ -\frac{1}{2} & 1 & -\frac{1}{2} & 0 & -\frac{\sqrt{3}}{2} \\ -\frac{1}{2} & -\frac{1}{2} & 1 & \frac{\sqrt{3}}{2} & 0 \\ -\frac{\sqrt{3}}{2} & 0 & \frac{\sqrt{3}}{2} & 1 & -\frac{1}{2} \\ \frac{\sqrt{3}}{2} & -\frac{\sqrt{3}}{2} & 0 & -\frac{1}{2} & 1 \end{bmatrix} \quad \text{(A1)}$$

References

[1] D. Ye, J. Li, J. Chen, R. Qu and L. Xiao, "Study on Steady-state errors for asymmetrical six-phase permanent magnet synchronous machine fault-tolerant predictive current control," *IEEE Transactions on Power Electronics*, vol. 35, no. 1, pp. 640-651, Jan. 2020.

[2] T. Tao, W. Zhao, Y. He, Y. Cheng, S. Saeed and J. Zhu, "Enhanced fault-tolerant model predictive current control for a five-phase PM motor with continued modulation," *IEEE Transactions on Power Electronics*, vol. 36, no. 3, pp. 3236-3246, Mar. 2021.

[3] X. Wang, Z. Wang, Z. Xu, W. Wang, B. Wang and Z. Zou, "Deadbeat predictive current control-based fault-tolerant scheme for dual three-phase PMSM drives," *IEEE Journal of Emerging and Selected Topics in Power Electronics*, vol. 9, no. 2, pp. 1591-1604, Apr. 2021.

[4] X. Wang, Z. Wang, M. Gu, et al., "Fault-tolerant control of common

electrical faults in dual three-phase PMSM drives fed by T-type three-level inverters," *IEEE Transactions on Industry Applications*, vol. 57, no. 1, pp. 481-491, Jan.-Feb. 2021.

[5] L. Xiao, L. Zhang, F. Gao and J. Qian, "Robust fault-tolerant synergetic control for dual three-phase PMSM drives considering speed sensor fault," *IEEE Access*, vol. 8, pp. 78912-78922, 2020.

[6] S. He, X. Sui, Z. Liu, M. Kang, D. Zhou and F. Blaabjerg, "Torque ripple minimization of a five-phase induction motor under open-phase faults using symmetrical components," *IEEE Access*, vol. 8, pp. 114675-114691, 2020.

[7] B. Chikondra, U. R. Muduli and R. K. Behera, "An improved open-phase fault-tolerant DTC technique for five-phase induction motor drive based on virtual vectors assessment," *IEEE Transactions on Industrial Electronics*, vol. 68, no. 6, pp. 4598-4609, Jun. 2021.

[8] Z. Li, L. Wu, Z. Chen, Y. Shi, L. Qiu and Y. Fang, "Single- and two-phase open-circuit fault tolerant control for dual three-phase PM motor without phase shifting," *IEEE Access*, vol. 8, pp. 171945-171955, 2020.

[9] H. Xu, W. Huang, F. Bu, H. Liu and X. Lin, "Control of five-phase dual stator-winding induction generator with an open phase," *IEEE Trans. Ind. Electron.*, vol. 66, no. 1, pp. 696-706, 2019.

[10] L. Wu, Y. Guo, X. Huang, Y. Fang and J. Liu, "Harmonic torque suppression methods for single-phase open-circuit fault-tolerant operation of PMSM considering third harmonic BEMF," *IEEE Transactions on Power Electronics*, vol. 36, no. 1, pp. 1116-1129, Jan. 2021.

[11] A. Tani, M. Mengoni, L. Zarr, et al., "Control of multiphase induction motors with an odd number of phases under open-circuit phase faults," *IEEE Trans on Power Electronics*, vol. 27, no. 2, pp. 565-577, 2012.

[12] Bermudez M, Gonzalez-Prieto I, Barrero F, et al., "Open-phase fault-tolerant direct torque control technique for five-phase induction motor drives," *IEEE Trans on Industrial Electronics*, vol. 64, no.2, pp. 902-911, 2017.

[13] G. Liu, L. Qu, W. Zhao, Q. Chen and Y. Xie, "Comparison of two SVPWM control strategies of five-phase fault-tolerant permanent-magnet motor," *IEEE Trans. Power Electron*., vol. 31, no. 9, pp. 6621-6630, 2016.

[14] H. M. Ryu, J. W. Kim, S. K. Sul, "Synchronous-frame current control of multiphase synchronous motor under asymmetric fault condition due to open phases," *IEEE Transactions on Industry Applications*, vol. 42, no. 4, pp. 1062-1070, 2006.

[15] H. S. Che, M. J. Duran, E. Levi, M. Jones, W. Hew, "Post-Fault operation of an asymmetrical six-phase induction machine with single and two isolated neutral points," *IEEE Trans.Power Electron.*, vol. 29, no. 10 ,pp. 5406-5416, 2014.

[16] H. Guzman, M. J. Duran, F. Barrero,et al., "Speed control of five-phase induction motors with integrated open-phase fault operation using model-based predictive current control techniques," *IEEE Transactions on Industrial Electronics*, vol. 61, no. 9, pp. 4474-4484, 2014.

[17] W. Wang, J. Zhang, M. Cheng and S. Li, "Fault-Tolerant Control of Dual Three-Phase Permanent-Magnet Synchronous Machine Drives Under Open-Phase Faults," in *IEEE Trans. Power Electron.*, vol. 32, no. 3, pp. 2052-2063, March 2017

[18] X. Wang, Z. Wang, Z. Xu, M. Cheng, W. Wang and Y. Hu, "Comprehensive Diagnosis and Tolerance Strategies for Electrical Faults and Sensor Faults in Dual Three-Phase PMSM Drives," *IEEE Trans. Power Electron.*, vol. 34, no. 7, pp. 6669-6684, July 2019

[19] W. Li, G. Feng, Z. Li, J. Tjong and N. C. Kar, "Multireference frame based open-phase fault modeling and control for asymmetrical six-phase interior permanent magnet motors," *IEEE Transactions on Power Electronics*, vol. 36, no. 10, pp. 11712-11725, Oct. 2021.

[20] X. Wang, Z. Wang, M. He, Q. Zhou, X. Liu and X. Meng, "Fault-tolerant control of dual three-phase PMSM drives with minimized copper loss," *IEEE Transactions on Power Electronics*, vol. 36, no. 11, pp. 12938-12953, Nov. 2021.

[21] J. Huang, P. Zheng, Y. Sui, J. Zheng, Z. Yin and L. Cheng, "Third harmonic current injection in different operating stages of five-phase PMSM with hybrid single/double layer fractional-slot concentrated winding," *IEEE Access*, vol. 9, pp. 15670-15685, 2021.

[22] Y. Hu, Z. Q. Zhu, and M. Odavic, "Torque capability enhancement of dual three-phase PMSM drive with fifth and seventh current harmonics injection," *IEEE Trans. Ind Appl.*, vol. 53, no. 5, pp. 4526-4535, Sept.-Oct. 2017

[23] B. Wang, J. Wang, A. Griffo and B. Sen, "Experimental assessments of a triple redundant nine-phase fault-tolerant PMA SynRM drive," *IEEE Trans. Ind Electron*., vol.66, no. 1, pp. 772-783, 2019.

[24] W. Huang, W. Hua, F. Chen, M. Hu and J. Zhu, "Model predictive torque control with SVM for five-phase PMSM under open-circuit fault condition," *IEEE Transactions on Power Electronics*, vol. 35, no. 5, pp. 5531-5540, May. 2020.

[25] X. An, G. Liu, Q. Chen, W. Zhao and X. Song, "Robust predictive current control for fault-tolerant operation of five-phase PM motors based on online stator inductance identification," *IEEE Transactions on Power Electronics*, vol. 36, no. 11, pp. 13162-13175, Nov. 2021.

[26] Y. Zhao , T. A. Lipo, "Space vector PWM control of dual three-phase induction machine using vector space decomposition," *IEEE Trans. Ind Appl*., vol. 31, no. 5, pp. 1100-1109, 1995.

ZHIFENG ZHANG was born in Huludao, Liaoning Province, China. He received B.Eng. degree in Automation, M.S. degree in Power Electronics and Power Drives and Ph.D. degree in Electrical Machines and Apparatus from Shenyang University of Technology, Shenyang, China. in 2004, 2007 and 2011.

He is currently an associate professor at School of Electrical Engineering in Shenyang University of Technology. His research interests are multi-phase permanent-magnet motor and drives.

YUE WU is currently pursuing the Ph.D. degree in Electrical Engineering from Shenyang University of Technology. His research interests are multi-phase permanent-magnet machines and drives.

HeQun Su received the M.Sc. degree with the School of Electrical Engineering, Shenyang University of Technology, Shenyang. His research interests include multi-phase permanent-magnet synchronous motor control.

QuanZeng Sun is currently pursuing the Ph.D. degree in Electrical Engineering from Shenyang University of Technology, Shenyang. His research interests include multi-phase permanent-magnet synchronous motor control.